

# Phases of the one-dimensional Bose-Hubbard model

Author: Jofre Vallès Muns.

Facultat de Física, Universitat de Barcelona, Diagonal 645, 08028 Barcelona, Spain.

Advisor: Bruno Juliá Díaz

**Abstract:** We study the ground state phases of the one-dimensional Bose-Hubbard model. To do so, we employ the infinite time evolving block decimation (iTEBD) method, a tensor network based algorithm, which enables us to obtain a good approximation of the ground state of an infinite one-dimensional lattice. This method allows us to characterize the different phases and the transition between them.

## I. INTRODUCTION

Since the experimental observation of a Bose-Einstein condensate in 1995 [1] the study of ultracold atomic systems has been incredibly important for understanding modern aspects of quantum many-body theory. Nowadays, the amount of experimental control over these systems makes them ideal platforms for testing and observing quantum properties in a controlled manner [2]. An important example of such systems is the Bose-Hubbard model. This one describes the behavior of interacting bosons at zero temperature in an optical lattice.

An interesting phenomena captured by this model is the transition between a Mott Insulator (MI) and a superfluid (SF) phase. This phase transition corresponds to a quantum phase transition, an interesting type of transition that appears at  $T = 0$ . It occurs as a result of a competition between different ground state phases when a physical parameter is tuned.

In particular, ultracold atomic systems can be trapped in a potential which limits their movement to only one dimension. This is known as a *cigar shaped* configuration, and has shown interesting behaviour different to the three-dimensional case [3].

In recent years, tensor network based methods have been widely used to study many-body quantum systems. Tensor networks can capture the relevant entanglement properties of these systems and characterize them to a deeper level. These methods are still extensively used and of research interest, making it a promising field in the nearby future [4].

## II. THEORETICAL BACKGROUND

The expression of the one-dimensional Bose-Hubbard (BH) Hamiltonian in the canonical ensemble can be written in terms of the creation and annihilation operators,  $\hat{a}_i, \hat{a}_i^\dagger$ :

$$H_{\text{BH}} = -J \sum_{i=1}^{M-1} (\hat{a}_i^\dagger \hat{a}_{i+1} + \hat{a}_{i+1}^\dagger \hat{a}_i) + \frac{U}{2} \sum_{i=1}^M \hat{n}_i (\hat{n}_i - 1), \quad (1)$$

where  $M$  is the number of sites,  $J$  is the tunneling strength and  $U$  the on-site interaction strength. The

index  $i$  represents a single site of the lattice, and  $\hat{n}_i$  is the particle number operator on this site  $i$ . The creation and annihilation operators follow the bosonic commutation relations and in this work we will focus on repulsive interactions ( $U > 0$ ).

We will be working in the real Fock space, so each state of this basis is represented by the number of particles in each site of the lattice, e.g.,  $|n_1, n_2, \dots, n_M\rangle$ .

The first term of the Hamiltonian (1) is the so-called *hopping* term, which enables a particle to tunnel between neighbouring sites. The second one is the interaction term and it accounts for the interaction between two atoms in the same lattice site.

When the tunneling dominates over the on-site interaction ( $J \gg U$ ) the system exhibits a superfluid (SF) phase, described by a wave function where all the particles are delocalized in the lattice. In the limit  $J/U \rightarrow \infty$ , the ground state wavefunction becomes,

$$|\psi_{\text{SF}}\rangle = \left( \frac{1}{\sqrt{N}} \sum_{i=1}^M \hat{a}_i^\dagger \right)^N |0\rangle. \quad (2)$$

On the other hand, when the on-site interaction dominates over the tunneling ( $J \ll U$ ), it appears the Mott Insulator (MI) phase, where all the particles are localized in the lattice sites. In this state there is no phase coherence between the particles. In the limit  $J/U \rightarrow 0$ , the ground state wavefunction reads,

$$|\psi_{\text{MI}}\rangle = \prod_{i=1}^M \left( \hat{a}_i^\dagger \right)^n |0\rangle, \quad (3)$$

where  $n = N/M$  is the so-called filling factor, which we take to be an integer number.

To study the phases of the BH we work in the grand canonical ensemble, so we consider our system in thermodynamic equilibrium with a reservoir of atoms. This is achieved adding to the original Hamiltonian a term of the form,

$$H = H_{\text{BH}} - \mu \sum_i \hat{n}_i, \quad (4)$$

where  $\mu$  is the chemical potential and gives preferent value to a certain amount of particles in the system.

Hence we have  $U$ ,  $J$  and  $\mu$  as the free parameters that determine the phase of the ground state. To characterize the phase diagram we fix  $U = 1$  and we modify  $J$  and  $\mu$ . The main goal of our work is to find the ground state of the system for different values of  $J/U$  and  $\mu/U$  and to determine to which phase it belongs.

A key concept in our work is the Schmidt decomposition of a state. If we consider a partition of the whole Hilbert space  $\mathcal{H} = \mathcal{H}_1 \otimes \mathcal{H}_2$ , the Schmidt decomposition enables us to write a pure state  $|\psi\rangle$  as the product of an orthonormal basis of  $\mathcal{H}_1$  ( $\{|\alpha\rangle_1\}$ ) and  $\mathcal{H}_2$  ( $\{|\alpha\rangle_2\}$ ), respectively;

$$|\psi\rangle = \sum_{\alpha=1}^d \Lambda_{\alpha} |\alpha\rangle_1 \otimes |\alpha\rangle_2, \quad (5)$$

where  $d = \min(\dim(\mathcal{H}_1), \dim(\mathcal{H}_2))$  and  $\Lambda_{\alpha}$  are the so-called Schmidt values which fulfill  $\sum_{\alpha} \Lambda_{\alpha}^2 = 1$ . As an example, if there is no entanglement between the two partitions, that is the state  $|\psi\rangle$  can be written as a product of the basis  $\{|\alpha\rangle_1\}$  and  $\{|\alpha\rangle_2\}$  ( $|\psi\rangle = |\psi\rangle_1 \otimes |\psi\rangle_2$ ), there is only one Schmidt value that is non-zero  $\Lambda_1 = 1$  [5]. This decomposition is useful to characterize the entanglement between different partitions in our system.

Another important quantity is the von Neumann entanglement entropy, which we can obtain from the Schmidt values,  $S = -\sum_{\alpha} \Lambda_{\alpha}^2 \log \Lambda_{\alpha}^2$ . It enables us to quantify the entanglement between the two chosen partitions of our system. When two partitions are not entangled the von Neumann entanglement entropy is zero,  $S = 0$ . The entanglement entropy can be used to determine the phases of the system. The MI state eq. (3) obtained in the limit  $J/U \rightarrow 0$  has no entanglement between two spatial partitions, thus  $S = 0$ . On the other hand, the SF state obtained in the limit  $J/U \rightarrow \infty$  is entangled,  $S \neq 0$ .

### III. NUMERICAL METHOD: MATRIX PRODUCT STATES

The exact diagonalization study of quantum many-body systems presents an important challenge in numerical computation since the dimension of the associated many-body Hilbert space grows exponentially fast [6] with the number of particles,  $N$ , and the number of sites in the lattice,  $M$ . This makes impractical to find the ground state for systems with more than  $N = 10$  bosons on  $M = 10$  sites.

It is in this context where Tensor Network (TN) algorithms play an important role in the modern simulation of quantum many-body systems. TN methods represent quantum many-body states as a product of tensors. This formalism allows to capture relevant entanglement properties of a system [4]. In particular, a matrix product state (MPS) describes the wave function of a one-dimensional system as a product of matrices.

TNs limit the amount of entanglement present in a system since they always fulfill an area law. This means that the entanglement entropy of these states grows proportionally with the size of the boundary between two partitions. This could seem a crude approximation for representing quantum states of many-body Hamiltonians since the entanglement entropy is upper bounded by a volume law, it grows with the volume of each partition. Nevertheless it is known that the low-energy states of gapped, local, frustration-free Hamiltonians in one-dimension fulfill an area law [7]. This makes TNs a very suitable representation of these systems since we will not work with the full Hilbert space. Instead, we will be constrained to the small region of it which fulfills the area law.

In an MPS [5], the wave function  $\psi$  of a pure quantum state is decomposed into products of matrices,

$$|\psi\rangle = \sum_{n_1, \dots, n_M} T_{\alpha_1 \alpha_2}^{[1]n_1} T_{\alpha_2 \alpha_3}^{[2]n_2} \dots T_{\alpha_M \alpha_{M+1}}^{[M]n_M} |n_1, \dots, n_M\rangle, \quad (6)$$

where  $M$  is the number of sites, there are  $\dim(n_i)$  matrices  $T^{[i]n_i}$  of dimension  $\chi_i \times \chi_{i+1}$  for each site  $i$ , and we are using Einstein notation, so we are summing over the repeated indices. We call this set of matrices  $T_{\alpha_i \alpha_{i+1}}^{[i]n_i}$  a rank-three tensor, its superscript  $[i]$  denotes the set of matrices in this particular  $i$  site, the subscripts  $\alpha_i \alpha_{i+1}$  are called *bond* or *virtual* (most of the time we will omit them) and the superscript  $n_i$  is called a *physical* index, since it refers to the site  $i$  in the Fock space.

It is important to note that in the MPS, the finite dimension  $\chi$  of the matrices  $T^{[i]n_i}$  is the beforementioned constrain that restricts the space to only the necessary part of the Hilbert space. This can be easily seen with the canonical representation of the MPS, where we rewrite the  $T^{[i]n_i}$  matrices,

$$|\psi\rangle = \sum_{n_1, \dots, n_M} \Lambda^{[1]n_1} \Gamma^{[1]n_1} \dots \Gamma^{[M]n_M} \Lambda^{[M+1]n_M} |n_1, \dots, n_M\rangle, \quad (7)$$

where  $\Lambda^{[i]}$  is a square, diagonal matrix with the Schmidt values on the diagonal. This Schmidt values of the site  $i$  are obtained from the Schmidt decomposition between the left and right sites of this site, hence the canonical representation is obtained with multiple Schmidt decompositions. Then, if we only have entanglement between the degrees of freedom near this site, we can truncate the  $\Lambda$  matrix up to a certain value since the Schmidt values will decrease quickly.

#### A. Time Evolving Block Decimation (TEBD)

The TEBD algorithm allows us to calculate the time evolution of a quantum state. For a typical quantum state this can be done with the time evolution operator  $U$ ,  $|\psi(t)\rangle = U(t)|\psi(0)\rangle$ , with  $U(t) = e^{-itH}$  (we are choosing units  $\hbar = 1$ ). If we define  $\tau \rightarrow -it$ , we can do an

imaginary time evolution with  $U(\tau) = e^{-\tau H}$ , which enables us to find the ground state of a Hamiltonian. Since the goal in our work is to characterize the ground state of the system, we are interested in the latter and we use this method with an initial random state to obtain the ground state.

We need to find the representation of this  $U$  operator in this MPS formalism. To do this, the TEBD algorithm uses the Suzuki-Trotter decomposition, where for a small  $\delta$  parameter it approximates the exponential of two operators  $X$  and  $Y$ ,  $e^{(X+Y)\delta} = e^{X\delta}e^{Y\delta} + \mathcal{O}(\delta^2)$ , and it assumes that the Hamiltonian can be expressed as a sum of two-site operators, so it can be decomposed as a sum on the odd sites and on the even sites. Using the Suzuki-Trotter decomposition the  $U$  operator reads,

$$U(dt) \simeq \left[ \prod_{i \text{ odd}} U^{[i,i+1]}(dt) \right] \left[ \prod_{i \text{ even}} U^{[i,i+1]}(dt) \right], \quad (8)$$

where now this  $U^{[i,i+1]}$  operator acts on only two sites. With the expression of the MPS, this can be understood as in order to do a single iteration of this operator, we first evolve between the odd sites and then we evolve between the even sites. This is considered as a single iteration of the time evolution.

To ensure that this evolution conserves the canonical form, we have to choose a small time step  $dt$  so the  $U$  operator makes a small change in the state. Since now we are evolving in imaginary time evolution the  $U$  operator is not unitary and with a big  $dt$  the canonical form will not be conserved. Thus, we repeatedly apply this operator with a small time step until we get a converged state. In each update, the dimension of the matrices will increase, and we will have to truncate them up to a value **trunc** (which is nothing else than the dimension of the matrices  $\chi$ ), which will define the entanglement between the states in the system. With a large value of **trunc**, the results better capture the entanglement in the system.

To obtain the quantities of the ground state, e.g., the energy per site, number of particles per site, etc, we need to find the representation of these operators as a sum of two-site operators and we apply them to the final state.

### B. Infinite Time Evolving Block Decimation (iTEBD)

The iTEBD algorithm is a generalization of the TEBD algorithm that allows to study infinite one-dimensional systems by exploiting the translational invariance of the Hamiltonian. It can be thought as the TEBD algorithm with open boundaries in the limit of number of sites  $M \rightarrow \infty$ . The basic idea of the algorithm is to first define a unit cell in the system that will be repeated infinitely many times. Then apply the time evolution operator over this unit cell. Translational invariance guarantees that all other unit cells will evolve in the same way and thus this cell will be able to describe the whole system.

In the Bose-Hubbard model, this unit cell will be only two sites (two  $\Lambda$  and two  $\Gamma$  tensors) since we have seen we can describe the Hamiltonian as a sum of local two-sites operators. This algorithm will be highly useful since it will enable us to simulate infinite systems with little computational work, as we will only need to keep evolving our unit cell until we reach the ground state. In the following we will employ this algorithm to obtain the ground state phase diagram of the Bose-Hubbard model.

This iTEBD and the standard TEBD algorithm were programmed following the notes from [8] with *Python* using the *Numpy* library for tensor contractions.

### C. Convergence of the results

In order to obtain the ground state for a particular value of  $\mu/U$  and  $J/U$ , we have three parameters which have to be tuned in order to obtain a proper convergence of the state: **steps**, **dt** and **trunc**. The two first are computational related and the latter is a physical parameter, which as previously explained captures the entanglement between two subsystems in the system.

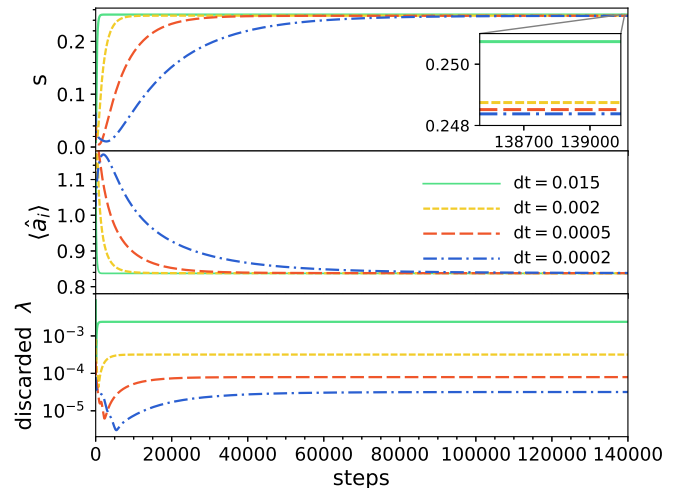


FIG. 1: Convergence of different quantities with the iTEBD algorithm for an increasing number of iterations with  $J/U = 0.2$ ,  $\mu/U = 0.6$  and **trunc**=3.

As previously stated, a small time step ( $dt$ ) is necessary in order to maintain the canonical form of our state, obtaining a better result as this value is reduced. This can be seen in Fig. 1, where we represent the order parameter  $\langle \hat{a}_i \rangle$ , the entanglement entropy per site  $s = S/M$  and the discarded  $\lambda$  per step (the amount of Schmidt values that are truncated in each step). This last amount is a useful quantity to characterize the error of the ground state at each time step, since it accounts for the values that are discarded; if this value is large, we might be *throwing* relevant information of the state. It is important to note that these figures are obtained with **trunc** = 3, hence we are doing an important truncation

of the entanglement properties and we are losing relevant information of the state as well.

As seen in the mentioned figure, a larger time step needs fewer iterations (**steps**) and consequently computational time, in order to obtain a converged result. As we explained, this is at the expense of relevant information, that can be captured by the error on the final obtained quantities. This error is shown in the zoomed plot in Fig. 1, where we can see that although the result is fully converged, there is a discrepancy between the results obtained with each  $\mathbf{dt}$ . Thus, a larger  $\mathbf{dt}$  has a certain error in the obtained quantities.

Also, the number of **steps** needed to obtain a converged result, changes significantly in the region of the phase space. More iterations are needed in the regions near the transition than in the center of the MI and SF phases. This forces us to keep track of the convergence and to make sure the result is converged.

#### IV. RESULTS

In this section we will focus on the results obtained with the explained iTEBD method. The quantities we compute are: The order parameter  $\langle \hat{a}_i \rangle$  which is non-zero in the SF phase and zero in the MI one; the mean particle number per site  $\langle \hat{n}_i \rangle$ ; the variance of the particle number operator per site  $\Delta \hat{n}_i$ ; the nearest-neighbour correlation  $\langle \hat{a}_i^\dagger \hat{a}_{i+1} \rangle_c = \langle \hat{a}_i^\dagger \hat{a}_{i+1} \rangle - \langle \hat{a}_i^\dagger \rangle \langle \hat{a}_{i+1} \rangle$ , which is zero when there is no spatial correlation; the von Neumann entanglement entropy per site  $s = S/M$  and the energy per site  $e = E/M$ .

We compute the results with  $\mathbf{trunc} = 3$ , so we are strongly limiting the entanglement in the system. Even though the small amount of entanglement it is enough to capture the SF to MI phase transition. The results in the *Phase diagram* subsection (IV B) are obtained with  $\mathbf{dt} = 0.015$  in order to obtain fast converged results, since we need to compute all the quantities for a large number of  $J/U$  and  $\mu/U$  values and the error due to the big  $\mathbf{dt}$  in the third decimal will not be relevant in the colormap plots. In subsection *Phase transition* (IV A), since we obtain the results with  $\mu/U$  fixed, we can do much more **steps** of the algorithm and we use  $\mathbf{dt} = 0.002$  to obtain better results.

##### A. Phase transition

We can see [11] in Fig. 2 that all the quantities show an abrupt change in their behaviour in  $J/U \simeq 0.105$ , manifesting the presence of the phase transition.

The value  $\langle \hat{a}_i \rangle$  will be the quantity we will use to characterize the two phases since it is clearly non-zero only on the SF phase. We can also see a local maximum in  $s$  and  $\langle \hat{a}_i^\dagger \hat{a}_{i+1} \rangle_c$  in the transition point. This signals the increase of quantum correlations at the phase transition.

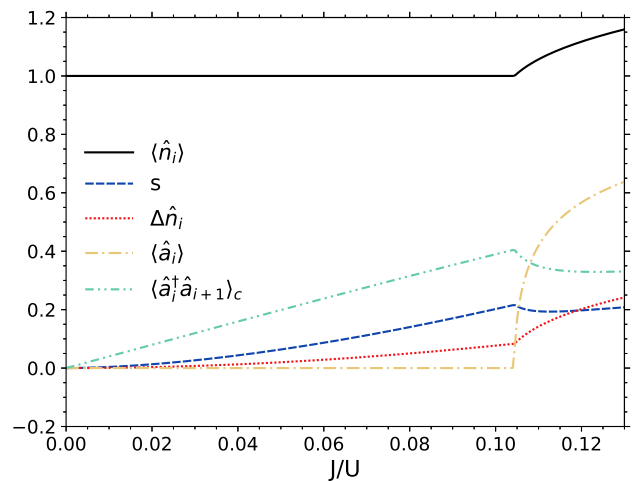


FIG. 2: Evolution of the different quantities described in the text as  $J/U$  is increased for  $\mu/U = 0.6$  and  $\mathbf{trunc}=3$ , where  $i$  represents an arbitrary site in the lattice. This figure reproduces Fig. 3a of [9].

##### B. Phase diagram

We now compute the quantities for a range of values of  $\mu/U$  and  $J/U$ , so we can obtain the phase diagram of the BH model, in which we can clearly differentiate the MI and SF phases.

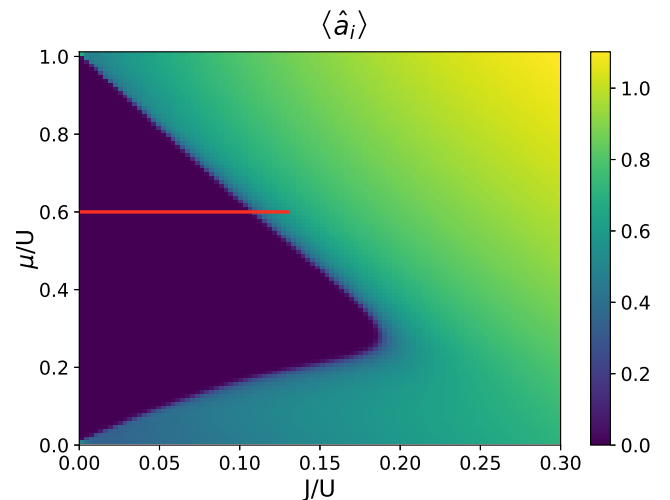


FIG. 3: Visualization of the first Mott lobe in the phase diagram for  $\mathbf{trunc}=3$ , where we represent the evolution of the order parameter  $\langle \hat{a}_i \rangle$  along the phase space. The red horizontal line shows the cut displayed by Fig. 2.

In Fig. 3 we represent the SF order parameter  $\langle \hat{a}_i \rangle$  in the phase space. In the figure we clearly see the MI region where  $\langle \hat{a}_i \rangle \simeq 0$  and the SF region where the order parameter is non-zero. The difference between both phases can also be seen in most of the plots in Fig. 4. This MI region in  $\mu/U \in [0, 1]$  is called the

first Mott lobe, and higher order Mott lobes can be obtained for  $\mu/U \in [1, 2]$ ,  $\mu/U \in [2, 3]$ , ... Mott lobes are characterized by  $\langle \hat{a}_i \rangle = 0$  and an integer value in the number of particles per site [10], going from  $\langle \hat{n}_i \rangle = 1$  for the first Mott lobe and getting increased by one unit for each succeeding Mott lobe. In the  $\langle \hat{n}_i \rangle$  plot in Fig. 4(c) we can see this  $\langle \hat{n}_i \rangle = 1$  filling, and in this same figure, in the plot of  $\Delta \hat{n}_i$  (d) we can also see that the variance in the number of particles per site in the Mott lobe is much smaller compared to the SF, coinciding with the limit mentioned in eq. (2) and (3).

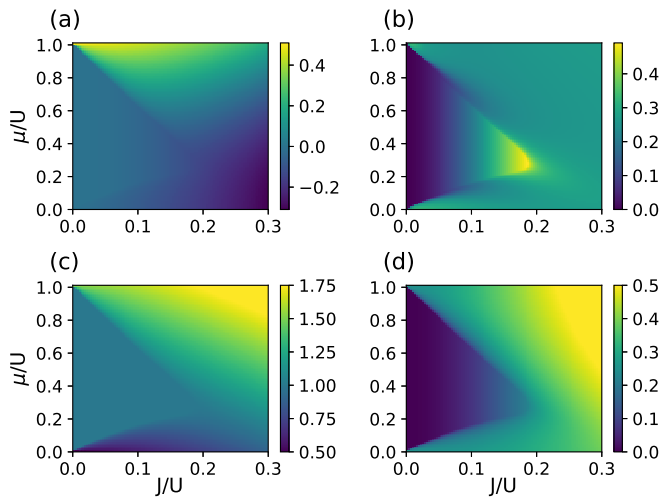


FIG. 4: Ground state properties of the system,  $e/U$  (a),  $s$  (b),  $\langle \hat{n}_i \rangle$  (c) and  $\Delta \hat{n}_i$  (d) as a function of the relevant parameters  $\mu/U$  and  $J/U$ . In all cases the truncation is set to `trunc=3`.

In this phase diagram we can also see the slight triangular shape of this Mott lobe. Bigger values of `trunc` would enable us to see how this shape sharpens and exhibits reentrance from the SF to the MI phase [9], but in our work we limit our simulations to small values of `trunc` and we consider it a good approximation to the BH model.

In Fig. 4(b) we can also see the so-called tip of the

Mott lobe in the entanglement entropy per site,  $s$ . This tip shows us a maximum in the entanglement entropy, where we can understand that our approximation with a low value of `trunc` will fail, being compatible with the beforementioned sharpening of the Mott lobe for bigger values of `trunc`.

## V. CONCLUSIONS

We have studied the phases of the one-dimensional Bose-Hubbard with the MPS formalism and the iTEBD algorithm. In doing so, we have characterized the entanglement of the system and we have benefited of the area law for the entanglement entropy verified by TNs, to obtain results impossible to obtain via the traditional exact diagonalization study.

We have also studied the convergence and applicability of the iTEBD algorithm. With the quantities we obtained, we characterized the MI and SF phases and the transition between them.

Both algorithms we programmed show a lot of potential to do further exploration in this system, it would be interesting to use the TEBD algorithm to analyze how the different quantities scale with the system size, in particular the entanglement entropy, enabling us to study the difference in scaling between the MI and SF phases.

Finally, this work has reflected the importance of tensor network algorithms in modern simulations of quantum many-body systems.

## Acknowledgments

I would like to thank Bruno Juliá and Ivan Morera not only for their guidance and help in the development of this work, but also for making it an extremely rewarding experience. I would also like to thank my family and friends for their immense support.

- 
- [1] M. H. Anderson, J. R. Ensher, M. R. Matthews, C. E. Wieman, and E. A. Cornell, *Science* **269**, 198-201 (1995).
  - [2] F. Schäfer, T. Fukuhara, S. Sugawa *et al.*, *Nat. Rev. Phys.* **2**, 411–425 (2020).
  - [3] L. Pitaevskii and S. Stringari, *Bose-Einstein Condensation and Superfluidity*, Oxford University Press (2016).
  - [4] R. Orús, *Ann. Phys. (N. Y.)* **349**, 117-158 (2014).
  - [5] J. Hauschild and F. Pollmann, *SciPost Phys. Lect. Notes* **5** (2018).
  - [6] J. M. Zhang and R. X. Dong, *Eur. J. Phys.* **31**, 591-602 (2010).
  - [7] M. B. Hastings, *J. Stat. Mech.: Theory Exp.* P08024 (2007).
  - [8] F. Pollmann, *Introduction to Matrix-Product States and Algorithms* [PowerPoint slides]. European Tensor Network (2016).
  - [9] M. Pino, J. Prior, A. M. Somoza, D. Jaksch and S. R. Clark, *Phys. Rev. A* **86**, 023631 (2012).
  - [10] M. P. A. Fisher, P. B. Weichman, G. Grinstein and D. S. Fisher, *Phys. Rev. B* **40**, 546 (1989).
  - [11] We detected an error in two quantities shown in the original figure we want to reproduce in [9], we already contacted the author but that is the reason why two quantities in this figure appear different from the reference.